Virology **303,** 287–296 (2002)
doi:10.1006/viro.2002.1601

Successful Protection by Amantadine Hydrochloride against Lethal Encephalitis Caused by a Highly Neurovirulent Recombinant Influenza A Virus in Mice

Isamu Mori,*,¶ Beixing Liu,* Md. Jaber Hossain,* Hiroki Takakuwa,‡ Tohru Daikoku,‡ Yukihiro Nishiyama,‡ Hironobu Naiki,† Kazuo Matsumoto,§ Takashi Yokochi,¶ and Yoshinobu Kimura*,[1]

*Department of Microbiology and †Department of Pathology, Fukui Medical University School of Medicine, Fukui 910-1193, Japan; ‡Laboratory of Virology, Research Institute for Disease Mechanism and Control, Nagoya University School of Medicine, Nagoya 466-8550, Japan; §Division of Microbiology, Fukui Prefectural Institute of Public Health, Fukui 910-8551, Japan; and ¶Department of Microbiology and Immunology, Aichi Medical University School of Medicine, Aichi 480-1195, Japan

Received June 19, 2001; returned to author for revision December 18, 2001; accepted May 30, 2002

A mouse model system for a lethal encephalitis due to influenza has been established by stereotaxic microinjection with the recombinant R404BP strain of influenza A virus into the olfactory bulb of C57BL/6 mice. The virus infection spread selectively to neurons in nuclei of the broad areas of the brain parenchyma that have anatomical connections to the olfactory bulb, leading to apoptotic neurodegeneration. The inflammatory reaction at the extended stage of viral infection involved the vascular structures affected by induction of inducible nitric oxide synthase and protein nitration; those were related to the etiology of fatal brain edema. The intraperitoneal administration of amantadine inhibited the viral growth in the brain and saved mice from the lethal encephalitis. The severity of neuronal loss paralleled the time lag between the virus challenge and the start of amantadine treatment. Thus, early pharmacological intervention is essential to minimize neurological deficits due to influenza virus-induced neurodegeneration.

Key Words: influenza virus; encephalitis; neurodegeneration; apoptosis; amantadine; nitric oxide; blood-brain barrier; olfactory system; limbic system.

INTRODUCTION

Infections with influenza virus, in some cases, precipitate acute encephalitis/encephalopathy especially in young children (Fujimoto *et al.,* 1998; Kasai *et al.,* 2000; Kolski *et al.,* 1998; McCullers *et al.,* 1999; Mizuguchi, 1997; Ryan *et al.,* 1999; Sugaya, 2000; Togashi *et al.,* 2000). This central nervous system (CNS) disease often leads to a lethal outcome or, if survived, severe neurological sequelae (Kasai *et al.,* 2000). One to two hundred children with this disorder are estimated to die during every influenza season in Japan (Okabe *et al.,* 2000). Thus, the elucidation of pathomechanisms of the influenza-associated encephalitis/encephalopathy appears urgent, and effective prophylactic and therapeutic strategies directed against this disease should be researched. However, information concerning such influenza virus-induced CNS disorders is extremely limited in the absence of appropriate animal models. Accumulating evidence has suggested the potential neuroinvasiveness of influenza virus for humans (Frankova *et al.,* 1977; Fujimoto *et al.,* 1998; Gamboa *et al.,* 1974; Hakoda and Nakatani, 2000; Hayase and Tobita, 1997; Ito *et al.,* 1999; McCullers *et al.,* 1999; Murphy and Hawkes, 1970; Takahashi *et al.,* 2000; Thraenhart *et al.,* 1975; Togashi *et al.,* 2000).

Recently, we reported on a nonlethal experimental virus-animal system where the neurovirulent WSN strain of influenza A virus, after being introduced into the olfactory bulb, targets several brain structures which are highly implicated in regulation of behavior and neuropsychiatric disturbances (Mori *et al.,* 1999). Infected neurons die through mechanisms associated with apoptosis (Mori and Kimura, 2000, 2001). Here we describe the successful protection conferred by intraperitoneal administration of amantadine hydrochloride against lethal acute encephalitis induced by the highly neurovirulent recombinant R404BP strain of influenza A virus (Takahashi *et al.,* 1995) in an experimental mouse system. From the evidence, it can be inferred that the early antiviral treatment with amantadine suppresses the progression of viral infection and inflammation, keeping neuronal loss to a minimum.

RESULTS

Clinical course

Stereotaxic microinjection with 10^5 plaque-forming units (PFU)/mouse of the R404BP virus into the right main

[1] To whom correspondence and reprints should be addressed at Department of Microbiology, Fukui Medical University School of Medicine, 23-3 Matsuoka-cho, Yoshida-gun, Fukui 910-1193, Japan. Fax: 81-776-61-8104. E-mail: ykimura@fmsrsa.fukui-med.ac.jp.

0042-6822/02 $35.00

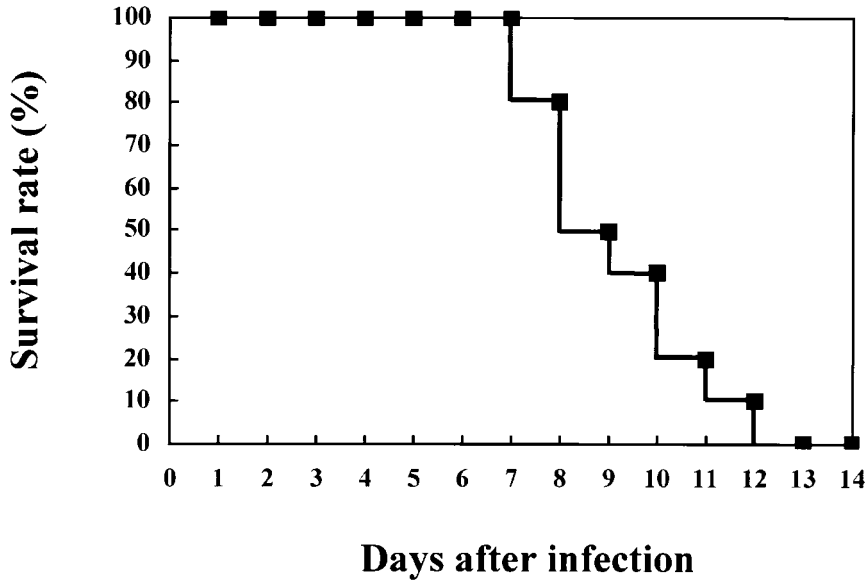

FIG. 1. Survival rate after infection with the recombinant R404BP strain of influenza A virus. The virus (10^5 PFU) was stereotaxically injected into the right olfactory bulb of C57BL/6 mice ($n = 10$).

olfactory bulb of C57BL/6 mice generated lethal acute encephalitis. The infected mice showed decreased motor activity, became emaciated, and died by day 13 (Fig. 1). Seizures were not provoked by the tail test. The limiting dilution study of the inoculum virus revealed that only one infectious R404BP virus particle was sufficient to kill a mouse in this experimental system, although the mean survival day (MSD) became prolonged (Table 1).

Spread of the R404BP virus in the mouse brain

To unveil the potential targets of the R404BP virus in the mouse brain, a large dose of the virus (10^5 PFU/mouse) was introduced into the olfactory bulb. On day 3 after infection, a large number of granule cells became infected along the needle track in the granular layer of the ipsilateral main olfactory bulb. Small clusters of infected neurons were found ipsilaterally in the anterior olfactory nucleus, tenia tecta, and piriform cortex. The virus also spread from the olfactory bulb, where the anterior tip of the lateral ventricle reaches, to the cerebral ventricle, a small number of ependymal cells being infected in the lateral and the third ventricles. Infiltration of mononuclear cells was not overt.

TABLE 1

Survival Rate after Microinjection with Various Doses of the R404BP Virus into the Right Olfactory Bulb of C57BL/6 Mice

Virus inoculum (log PFU)	Survival rate (survivor/total)	Mean survival day[a]
5	0/3	9.0 ± 0.5
4	0/3	8.0 ± 0.5
3	0/3	10.3 ± 0.5
2	0/3	10.7 ± 0.7
1	0/3	12.0 ± 0.8
0	0/3	14.3 ± 2.1
−1	3/3[b]	—

[a] Data are expressed as average ± SEM.
[b] Mice were clinically monitored for 28 days after the virus challenge.

On day 7 after the challenge, the virus targeted several brain structures which are directly connected to the main olfactory bulb. The virus infected most granule and mitral cells in the main olfactory bulb bilaterally, resulting in efficient transmission of the virus to the olfactory, limbic, and other brain structures coupled with the olfactory bulb. Thus, clusters of infected neurons were found in the tenia tecta, indusium griseum, cingulate cortex, the anterior olfactory nuclei, piriform cortex, hypothalamus, horizontal limb of the diagonal band, lateral mammillary nucleus, amygdaloid complex, raphe, and locus coeruleus (Figs. 2 and 3). Furthermore, the virus infection extended to the ventral tegmental area, substantia nigra, and oral reticular pontine nucleus. The virus heavily attacked some circumventricular structures, including the medial habenular nucleus (Fig. 2). These results revealed the increased neuroinvasive ability of the R404BP virus as compared with the original WSN virus (Mori *et al.,* 1999). At this time point, infected neurons began to shrink and neurites displayed a bead-like staining pattern, which can be explained by the process of neurodegeneration. The cresyl violet staining method disclosed shrunken neurons with peculiar nuclei in virus-infected regions of the brain. Neurons infected with the R404BP virus showed the terminal deoxynucleotidyl transferase-mediated dUTP nick end-labeling (TUNEL)-positive signals in a nuclear pattern, indicating that in-

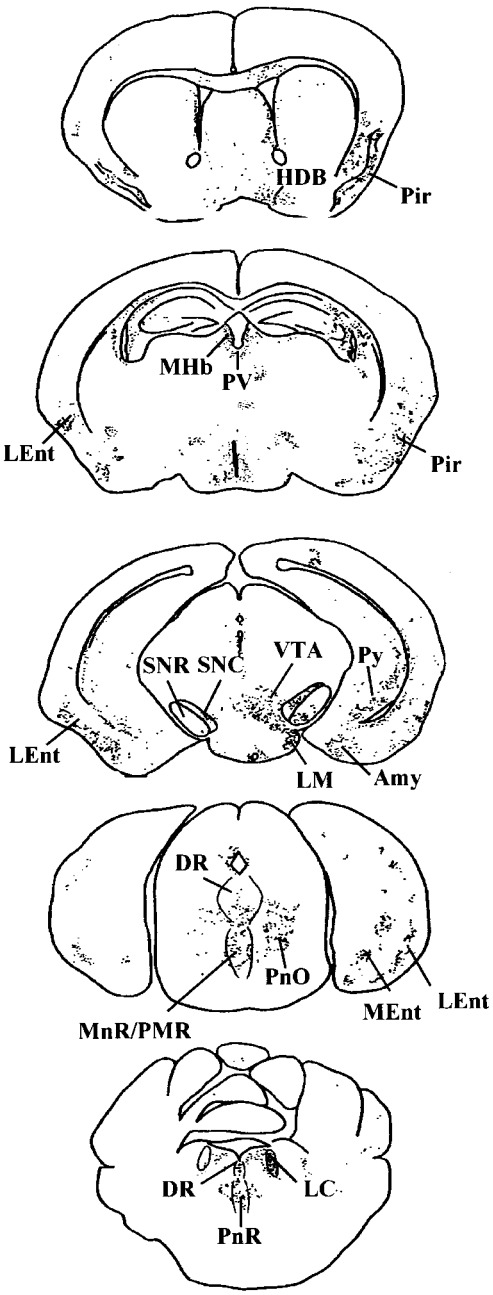

FIG. 2. Diagram of the distribution of virally infected neurons in anteroposterior coronal sections through the brain of C57BL/6 mice on day 7 after microinjection with the R404BP virus into the right olfactory bulb. Camera lucida illustrations show infected neurons, plotted at various levels of the brain. Abbreviations: Amy, amygdaloid complex; DR, dorsal raphe; HDB, nucleus of the horizontal limb of the diagonal band; LC, locus coeruleus; LEnt, lateral entorhinal cortex; LM, lateral mammillary nucleus; MEnt, medial entorhinal cortex; MHb, medial habenular nucleus; MnR, median raphe nucleus; Pir, piriform cortex; PMR, paramedian raphe nucleus; PnO, pontine reticular nucleus, oral; PnR, raphe pontis; PV, paraventricular thalamic nucleus; Py, pyramidal cell layer of the hippocampus; SNC, substantia nigra, compact; SNR, substantia nigra, reticular; VTA, ventral tegmental area.

fected neurons were dying through mechanisms associated with apoptosis (Fig. 4A). On day 9 after being infected with the R404BP virus, the topological distribution of the virus antigens resembled that of day 7. However, infected neurons further shrank and fissured into small bodies. Overall, the virus distribution patterns on day 4 and 10 after the challenge with 10 PFU of the virus corresponded to those on day 3 and 7 after infection with 10^5 PFU, respectively.

The postmortem study on day 10 showed heavy neuronal loss in the brain regions targeted by the virus (Fig. 4B). All postmortem brains on days 8, 9, 10, 11, and 12 showed brain edema, while the live brains on day 8, 9, and 10 did not, suggesting that the brain edema is the final death-determining factor (Figs. 4C and 4D).

Microinjection of the ultraviolet-inactivated R404BP virus into the right main olfactory bulb did not produce encephalitis.

In situ detection of iNOS and NT in the brain after infection with the R404BP virus

Because nitric oxide (NO) plays a pivotal role in cytotoxic activities and tissue damage during inflammatory processes (Reiss and Komatsu, 1998), we investigated brain slices for inducible nitric oxide synthase (iNOS) and nitrotyrosine (NT), an *in vitro* marker of NO-derived peroxynitrite. The immunohistochemistry did not detect iNOS and NT in the normal brains. The iNOS induction and nitration of tyrosine occurred in the virus-infected areas of the brain as early as 5 days after infection with 10^5 PFU of the virus, involving vessels on occasion (Fig. 5). Overall, distribution of the virus, mononuclear cell infiltration, iNOS, and NT coincided with each other. As infection progressed with time (on days 7 and 9), such vessels immunopositive for iNOS and NT increased in frequency, and the destruction of vascular structures manifested itself.

Systemic histopathological findings

The postmortem examination of the lungs of virus-infected mice showed mild alveolar hemorrhage without obvious inflammatory response. The heart, liver, kidney, and adrenal glands appeared congested. Representative lymphoid organs, including the thymus, spleen, and mesenteric lymph nodes, became atrophic and exhibited a number of apoptotic bodies. However, the polymerase chain reaction did not detect the influenza virus matrix gene in the blood samples collected on days 3, 6, and 9 after infection. The immunohistochemistry did not detect viral antigens in these organs collected on days 5, 7, and 9. These results suggest the absence of hematogenous dissemination of the virus during the course of the CNS infection.

Protective and therapeutic effects of amantadine hydrochloride

In an attempt to protect mice against the lethal acute encephalitis caused by the R404BP virus, we treated

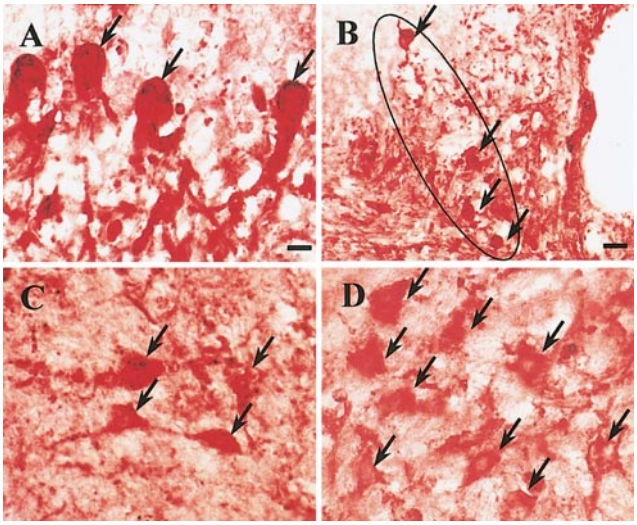

FIG. 3. Photomicrographs illustrating brain structures heavily attacked by the R404BP virus. (A) The mitral cell layer of the main olfactory bulb. Arrows point to the R404BP virus-infected mitral neurons. (B) Infected neurons (arrows), packed in a small area of the indusium griseum (surrounded by the elliptic line). (C) Infected neurons (arrows) in the nucleus of the horizontal limb of the diagonal band. (D) Infected neurons (arrows) in the substantia nigra, compact. The scale bar in (A) represents 10 μm, common to (C) and (D), while that in (B) indicates 20 μm.

mice with amantadine hydrochloride according to the prophylactic and therapeutic regimens (Table 2). Intraperitoneal administration of amantadine (100 mg/kg) transiently decreased motor activities of normal C57BL/6 mice as described previously (Messiha, 1989). The increase of the dose of amantadine to 200 mg/kg killed 100% of the mice within 3 min ($n = 6$). When mice were challenged with 10^5 PFU of the R404BP virus, amantadine administration based on the prophylactic regimen 1 (100 mg/kg, twice a day) did not confer protective effects (Table 2). However, when mice were infected with 10 PFU of the virus, treatment with the prophylactic regimen 1 completely protected mice against the acute encephalitis. No infected neurons appeared in the brain and all mice survived the infection. The prophylactic regimen 2 (100 mg/kg, once a day) appeared slightly effective in protecting mice against the acute encephalitis.

Therapeutic regimens 1 and 2 provided 100% survival (Table 2), although a small number of neurons became infected (Figs. 6A and 6B), displaying morphological alterations characteristic of apoptosis (Fig. 7A). The therapeutic regimen 3 resulted in a survival effect with statistic significance, although numerous neurons were infected (Fig. 6C). Therapeutic regimen 4 yielded no benefit at all; it did not prevent death of the animals nor extend

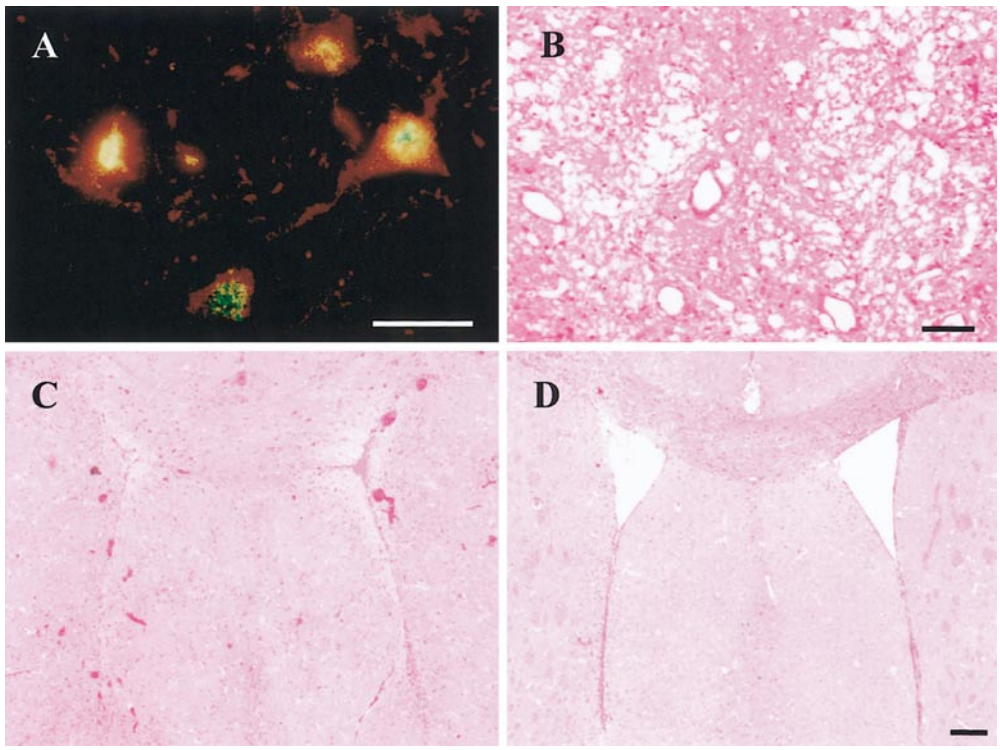

FIG. 4. Outcome of the CNS infection induced by the R404BP virus. (A) Confocal laser scanning microscopy of neurons in the anterior olfactory nucleus on day 7 after infection with the R404BP virus, illustrating evidence of apoptosis. The virus-specific signal is shown as red, the TUNEL-specific signal is shown as green, and the overlap of both as is shown as yellow. The scale bar represents 10 μm. (B) Heavy neuronal loss found in the MnR/PMR of the postmortem brain on day 10 after infection. Hematoxylin and eosin staining. The scale bar represents 50 μm. (C) The postmortem brain dissected from a mouse found dead on day 10 after infection. (D) The live brain obtained from a moribund mouse on day 10 after infection. The scale bar in (D) represents 100 μm, common to (C) and (D).

MSD (therapeutic regimen 4, 11.8 ± 0.8; PBS control, 12.4 ± 0.7; shown as average ± SEM).

Protective mechanism of the amantadine administration against the lethal encephalitis

We have examined the relationship between virus infection and NO-mediated nitration of proteins, especially focusing on involvement of capillaries in the mouse brain. When virally infected mice were treated according to therapeutic regimens 1 and 2, the immunohistochemistry did not detect iNOS or NT (Fig. 7B) in the brain. Inflammatory cell infiltration and brain edema were not evident. When mice underwent therapy on the basis of the therapeutic regimen 3, vascular structures remained almost free from viral infection (Fig. 7C), iNOS, protein nitration (Fig. 7D), and mononuclear cell infiltration. Again, brain edema was not found in these mice. In brains of virus-infected mice that were treated with PBS instead of amantadine, where virus invasion, protein nitration, and mononuclear cell infiltration appeared prominent, destruction of capillary structures was evident (Figs. 7E and 7F). Postmortem brains on day 10 showed brain edema.

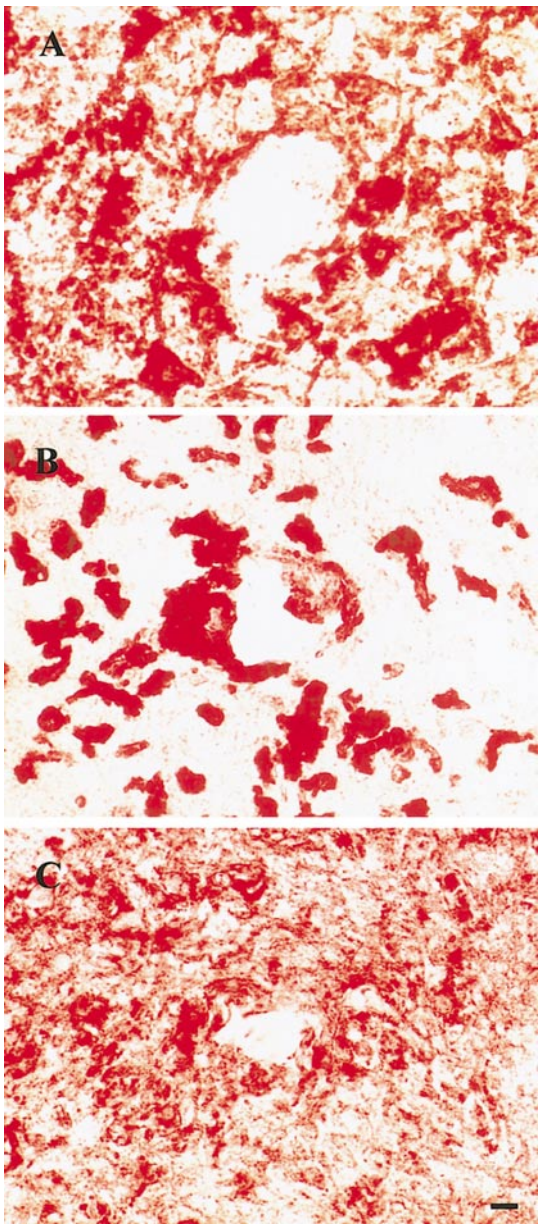

FIG. 5. Detection of iNOS and NT in the brain on day 5 after infection with the R404BP virus. In the VTA, a number of neurons became infected (A). Infection involved the vessel wall as well as the brain parenchyma. Detection of iNOS (B) and NT (C) in the corresponding area of consecutive brain slices. The scale bar represents 10 μm, common to (A) and (C).

TABLE 2

Prophylactic and Therapeutic Administration of Amantadine Hydrochloride against the Lethal Encephalitis Induced by the R404BP Virus

Protocol	Virus inoculum (log PFU)	Survival rate (survivor/total)
Prophylactic regimen 1[b]	5	1/5 (0/5)[a]
Prophylactic regimen 1	1	5/5 (0/5) $P < 0.005$[c]
Prophylactic regimen 2[d]	1	3/5 (0/5)
Therapeutic regimen 1[e]	1	5/5 (0/5) $P < 0.005$
Therapeutic regimen 2[f]	1	5/5 (0/5) $P < 0.005$
Therapeutic regimen 3[g]	1	4/5 (0/5) $P < 0.05$
Therapeutic regimen 4[h]	1	0/5 (0/5)
Control for amantadine toxicity[i]	—	3/3

[a] Control mice were intraperitoneally injected with PBS instead of amantadine hydrochloride solution.

[b] Prophylactic regimen 1: mice were intraperitoneally administered amantadine hydrochloride solution (100 mg/kg) twice a day (every 12 h) from day −1 (before infection) to day 11 after infection.

[c] Statistically significant by the Fisher's exact probability test.

[d] Prophylactic regimen 2: mice were intraperitoneally administered amantadine hydrochloride solution (100 mg/kg) once a day (every 24 h) from day −1 to day 11 after infection.

[e] Therapeutic regimen 1: mice were intraperitoneally administered amantadine hydrochloride (100 mg/kg) twice a day (every 12 h) from day 1 to day 12 after infection.

[f] Therapeutic regimen 2: mice were intraperitoneally administered amantadine hydrochloride (100 mg/kg) twice a day (every 12 h) from day 4 to day 15 after infection.

[g] Therapeutic regimen 3: mice were intraperitoneally administered amantadine hydrochloride (100 mg/kg) twice a day (every 12 h) from day 7 to day 18 after infection.

[h] Therapeutic regimen 4: mice were intraperitoneally administered amantadine hydrochloride (100 mg/kg) twice a day (every 12 h) from day 10 to day 21 after infection.

[i] Uninfected mice were treated with amantadine hydrochloride according to prophylactic regimen 1.

Neuronal loss in the brain of virus-infected mice

Neuronal loss on day 28 after infection was not evident in the brain of mice treated with prophylactic regimen 1 and therapeutic regimens 1 and 2 (Fig. 8A), while with the therapeutic regimen 3 a number of neurons disappeared from the brain (Fig. 8B).

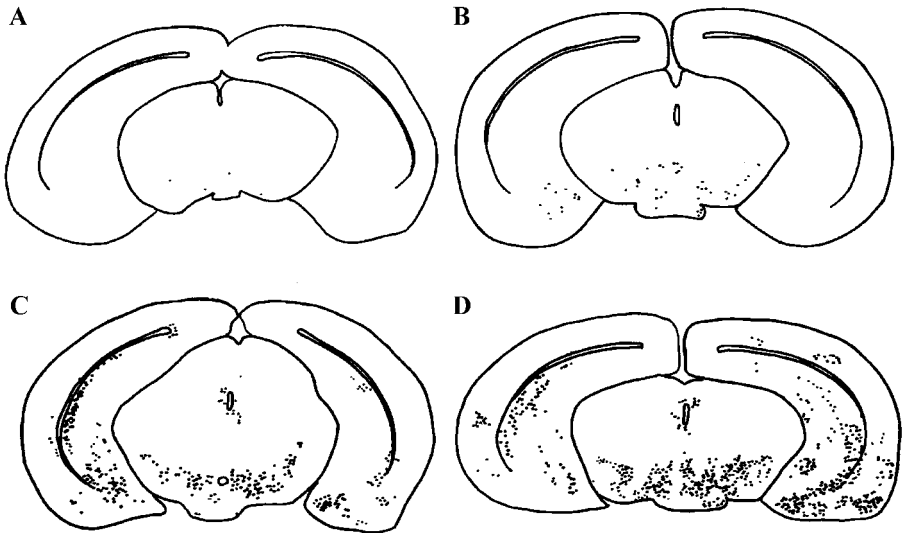

FIG. 6. Therapeutic effects of intraperitoneal administration of amantadine hydrochloride on the distribution of neurons infected with the R404BP virus. Camera lucida illustrations show infected neurons, plotted at the level of SNC/VTA on day 10 after infection. Mice were treated with amantadine according to therapeutic regimen 1 (A), therapeutic regimen 2 (B), and therapeutic regimen 3 (C). Control mice were injected with PBS instead of amantadine solution (D).

DISCUSSION

The present study establishes that the recombinant R404BP strain of influenza A virus presents an increased neuroinvasiveness in the mouse brain compared with the original WSN virus and that prophylactic and early therapeutic administration of amantadine protects mice against the lethal encephalitis induced by the R404BP virus.

The recombinant virus infects most granule cells (interneurons) and mitral cells (output neurons) in the main olfactory bulb, which enables the virus to efficiently attack a broad spectrum of targets which are directly linked to the olfactory bulb through the axonal pathways. It should be noted that there exists dense dentrodendritic synaptic interaction between granule and mitral cells (Price and Powell, 1970), providing explanation for the efficient viral transmission from granule to mitral cells. Thus, infected neurons are distributed in areas reciprocally connected to the olfactory bulb, such as the anterior olfactory nucleus, tenia tecta, and entorhinal cortices (Shipley and Adamek, 1984). Infection also progresses to areas that receive the olfactory bulb efferent, such as the indusium grisium (Adamek *et al.,* 1984), and areas that provide axonal projections to the olfactory bulb, such as the diagonal band, dorsal raphe, and locus coeruleus (Shipley and Adamek, 1984). Furthermore, the virus infection extends to structures directly coupled with some of the abovementioned primary targets, including the ventral tegmental area, substantia nigra, and oral pontine reticular nucleus (Oades and Halliday, 1987; Pasquier *et al.,* 1977; Shammah-Lagnado *et al.,* 1987). Thus, the increased neurovirulence of the R404BP virus, compared with the WSN virus, might be attributable to its ability to perform efficient transsynaptic transmission in the brain, as reported in herpes simplex and rabies viruses (Dehal *et al.,* 1993; Etessami *et al.,* 2000). It should be emphasized that selectivity of virus targeting is still retained despite the increased neuroinvasive potentiality of the virus. On the other hand, infection with the R404BP virus frequently involves vessels where peroxynitrite-mediated protein nitration takes place, leading to the disruption of the blood-brain barrier and the fatal brain edema.

Amantadine represents influenza A virus-specific antiviral action and has been used for prophylaxis and treatment of influenza A virus infection of the respiratory tract (Oxford and Galbraith, 1980). The primary antiviral action of amantadine derives from blocking the H^+ channel formed by the virion-associated M2 protein, prohibiting the flow of H^+ from the acidified endosome into the virion, an essential step for the release of the transcriptionally active ribonucleoprotein complex into the cytoplasm, i.e., the uncoating process. Amantadine is transported principally across the cerebral capillaries by a carrier-mediated transport system (Spector, 1988), which makes it possible for this drug to exert its antiviral actions in the brain parenchyma following the intraperitoneal administration. In our experimental system, amantadine therapy primarily inhibits viral growth in the neurons and consequently protects vessels from the inflammatory damages. It is highly likely that such secondary vasoprotection conferred by the amantadine treatment maintains the integrity of the blood-brain barrier, hindering the occurrence of brain edema and death of the animals.

The degree of neuronal depletion depends on the time

lag between the virus challenge and the start of amantadine treatment. Amantadine appears to have no effect on suppressing influenza virus infection, once the uncoating step has proceeded in each neuron. Interestingly, according to therapeutic regimens 1 and 2, inflammatory cells do not emerge in the brain regions where virally infected apoptotic neurons remain during amantadine treatment. In general, apoptosis does not result in a loss of cellular contents into the extracellular space, nor does it incite an inflammatory response, which sharply contrasts with necrosis (Bredesen, 1995). However, amantadine administration at a later stage of infection, based on therapeutic regimen 3, cannot control the progression of inflammation in the brain. Collectively, early pharmacological intervention is definitely important to minimize neuronal depletion due to the influenza virus infection and accompanying inflammation in the CNS.

Sequence analysis of the RT-PCR-amplified M2 region of influenza viruses revealed that amino acid sequence of the R404BP virus (data not shown) is exactly identical with that of the WSN strain, containing asparagine at position 31 (Markushin *et al.,* 1988). The amino acid residue at this position plays a definite role in susceptibility of the virus to the drug amantadine (Takeda *et al.,* 2002). The 50% inhibitory concentration of amantadine for the R404BP virus growth in MDCK cells *in vitro* was calculated as 1 μg/ml that indicates the virus strain used in the present study is less susceptible to the drug. It might be expected that more promising prophylactic and therapeutic virtue of amantadine *in vivo* could be attained in the case of infection with the ordinary drug-sensitive strains of influenza virus.

The induction of iNOS, which brings about overproduction of NO, may be beneficial to host defense against bacteria and parasites (James, 1995; Umezawa *et al.,* 1997). Likewise, the expression of iNOS has been documented in various viral infections, the significance of which still remains unsettled. Viruses can be both sensitive or resistant to the antiviral effects of NO, demonstrated in *in vitro* and *in vivo* experimental systems (Reiss and Komatsu, 1998). On the other hand, overproduction of NO, especially its oxidized intermediate, peroxynitrite, has been implicated in the pathophysiology of numerous inflammatory diseases (Morikawa *et al.,* 1999). Peroxynitrite is a highly reactive chemical that causes nitration and hydroxylation of tyrosine and tryptophan, as well as DNA injury. Administration of a competitive NOS inhibitor, L-NMMA, resulted in amelioration of influenza virus-induced pneumonia, suggesting a role of NO in viral pathogenesis (Akaike *et al.,* 1996). Thus, it could be interesting to investigate the pathological significance of iNOS induced in the brain after infection with the R404BP virus by manipulating NOS with its inhibitors and by using iNOS-deficient mice. Intriguingly, NO exerts both proapoptotic and antiapoptotic functions (Billiar, 2000). Roles played by NO in modulating cell viability should be investigated in this experimental system.

MATERIALS AND METHODS

Experimental virus-animal system

Specific pathogen-free female C57BL/6 mice, at the age of 4 weeks, were used for the experiments (Clear Japan, Osaka, Japan). The R404BP strain of recombinant influenza A virus was a kind gift from Dr. Setsuko Nakajima (The Institute of Public Health, Tokyo, Japan). The virus possesses the neuraminidase and matrix genes from the WSN virus (H1N1) and the rest from the non-neurovirulent A/Aichi/2/68 strain (H3N2). The original recombinant virus (R404 virus) had been passaged successively in the mouse brain and then a highly neurovirulent strain (R404BP virus) was isolated. Stereotaxic microinjection of the virus into the olfactory bulb was carried out as described previously (Mori *et al.,* 1999). Infected mice were clinically and histopathologically monitored daily after infection. An MSD was calculated according to the formula: $\mathrm{MSD} = \sum [f(d-1)]/N$, where f is the number of mice recorded dead on day d and N is the number of mice in a group (Grunert *et al.,* 1965). For virus inactivation, the virus suspension was exposed to a 15 W ultraviolet lamp at a distance of 15 cm at 4°C for 30 min with continuous and gentle stirring. After irradiation, infectivity was reduced to $<10^{-7}$ of the original.

Tissue processing and immunohistochemistry

The animals were anesthetized with an overdose of 7.2% chloral hydrate in phosphate-buffered saline (PBS) and perfused transcardially with 3.7% formaldehyde in PBS. The brains were removed, soaked in 15% sucrose in PBS at 4°C overnight, and frozen at −80°C. Coronal sections were cut at 14-μm-thickness on a cryostat. Postmortem organs were paraffin-embedded and cut on a microtome. Immunohistochemistry was performed as reported previously (Mori and Kimura, 2000) by using the rabbit polyclonal anti-WSN virus antibody (a generous gift from Dr. Setsuko Nakajima, The Institute of Public Health, Tokyo, Japan), rabbit polyclonal anti-iNOS antibody (Upstate Biotechnology, Lake Placid, NY; working concentration, 5 μg/ml), and rabbit polyclonal anti-nitrotyrosine antibody (Upstate Biotechnology; working concentration, 20 μg/ml). Goat anti-rabbit immunoglobulins conjugated to peroxidase-labeled dextran polymer in Tris–HCl buffer (DAKO Envision+, DAKO, Carpinteria, CA) was adopted as a secondary antibody.

Detection of apoptosis

Morphological alterations characteristic of apoptosis were investigated by the cresyl violet staining method. DNA fragmentation was detected *in situ* by the TUNEL method using an Apoptag Direct *in situ* apoptosis detec-

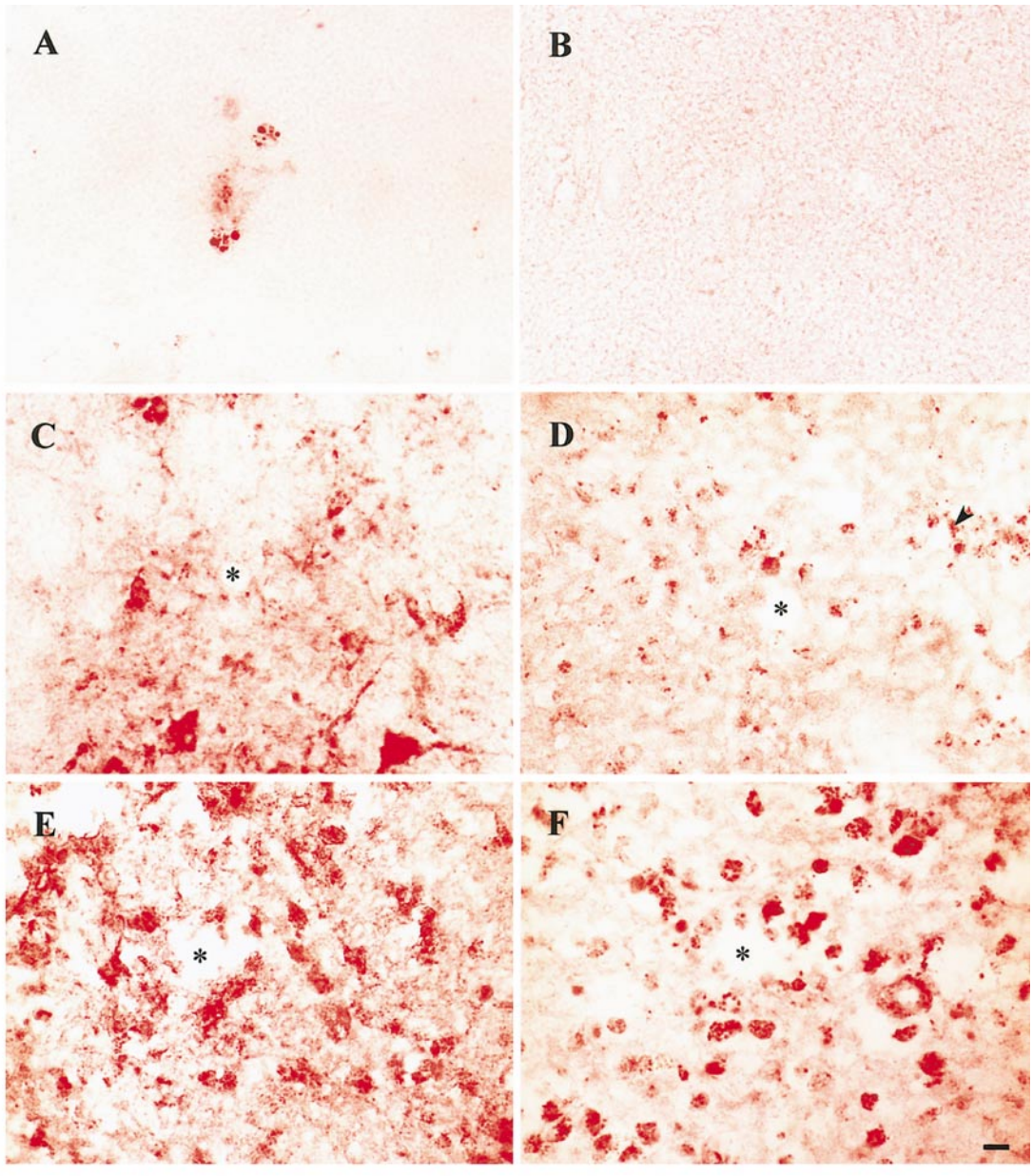

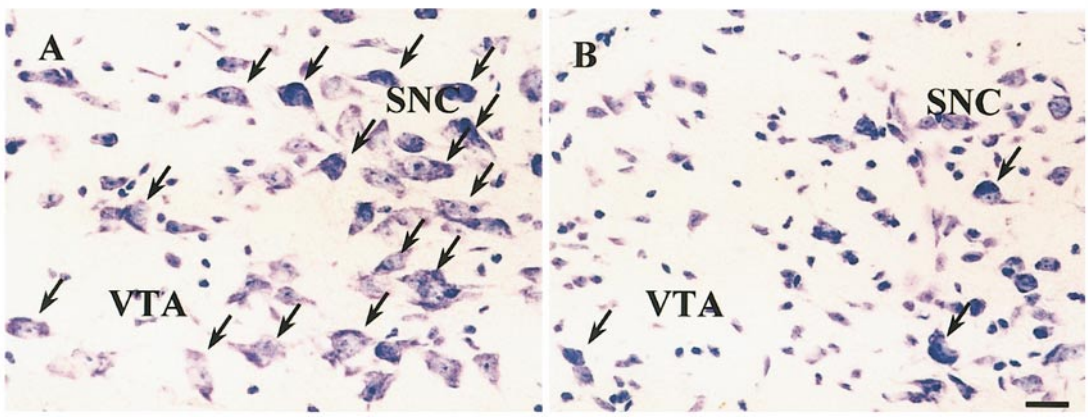

FIG. 7. Vascular histopathology of mice suffering from acute encephalitis induced by the R404BP virus. Mice were treated with the drug according to therapeutic regimen 1 (A and B) and therapeutic regimen 3 (C and D). Control mice received PBS (E and F). Brain slices were immunostained for virus antigens (A, C, and E) and for nitrotyrosine (B, D, and F). All samples were taken on day 10 after infection. The asterisks indicate vessel lumens. The scale bar represents 10 μm, common to A to F.

tion kit (Oncor, Gaithersburg, MD) as described in the previous article (Mori and Kimura, 2000).

Detection of the influenza virus gene

Total RNA was extracted from the blood samples by using the TRIZOL Reagent (Invitrogen, Carlsbad, CA). Glycogen (Invitrogen) was added to the samples to promote RNA precipitation. The cDNA synthesis and the successive polymerase chain reaction (PCR) were carried out with SUPERSCRIPT One-Step RT-PCR with PLATINUM *Taq* System (Invitrogen) according to the manufacturer's instructions with modifications. The cDNA was generated at 50°C for 30 min with the sense primer (5′-GAGATCGCACAGAGA-3′) (Urabe *et al.,* 1993). Then, the antisense primer (5′-TCGTTGCATCTGCAC-3′) (Urabe *et al.,* 1993) was added into the reverse transcription product. The PCR was performed with the schedule of 94°C for 3 min followed by 35 cycles of 94°C for 30 s, 56°C for 30 s, and 72°C for 1 min. The final products were differentiated on 1% agarose gel, stained with ethidium bromide, and visualized under an ultraviolet lamp.

Administration of amantidine

Amantadine hydrochloride (Sigma, St. Louis, MO) was intraperitoneally injected into the mice at a concentration of 10 mg/ml in sterile water, according to the protocol for the prophylactic and therapeutic regimens (Table 2). Mice were observed clinically and subjected to histopathological investigations after the virus challenge.

The concentration of amantadine that causes a 50% inhibition of the R404BP virus growth in MDCK cells *in vitro* was 1 μg/ml.

ACKNOWLEDGMENT

The authors thank Nobuo Takimoto for technical assistance with tissue preparation.

REFERENCES

Adamek, G. D., Shipley, M. T., and Sanders, M. S. (1984). The indusium griseum in the mouse: Architecture, Timm's histochemistry and some afferent connections. *Brain Res. Bull.* **12,** 657–668.

Akaike, T., Noguchi, Y., Ijiri, S., Setoguchi, K., Suga, M., Zheng, Y. M., Dietzschold, B., and Maeda, H. (1996). Pathogenesis of influenza virus-induced pneumonia: Involvement of both nitric oxide and oxygen radicals. *Proc. Natl. Acad. Sci. USA* **93,** 2448–2453.

Billiar, L. J. (2000). The role of nitric oxide in apoptosis. *Semin. Perinatol.* **24,** 46–50.

Bredesen, D. E. (1995). Neural apoptosis. *Ann. Neurol.* **38,** 839–851.

Dehal, N. S., Dekaban, G. A., Krassioukov, A. V., Picard, F. J., and Weaver, L. C. (1993). Identification of renal sympathetic preganglionic neurons in hamsters using transsynaptic transport of herpes simplex type 1 virus. *Neuroscience* **56,** 227–240.

Etessami, R., Conzelmann, K. K., Fadai-Ghotbi, B., Natelson, B., Tsiang, H., and Ceccaldi, P. E. (2000). Spread and pathogenic characteristics of a G-deficient rabies virus recombinant: An *in vitro* and *in vivo* study. *J. Gen. Virol.* **81,** 2147–2153.

Frankova, V., Jirasek, A., and Tumova, B. (1977). Type A influenza: Postmortem virus isolations from different organs in human lethal cases. *Arch. Virol.* **53,** 265–268.

Fujimoto, S., Kobayashi, M., Uemura, O., Iwasa, M., Ando, T., Katoh, T., Nakamura, C., Maki, N., Togari, H., and Wada, Y. (1998). PCR on cerebrospinal fluid to show influenza-associated acute encephalopathy or encephalitis. *Lancet* **352,** 873–875.

Gamboa, E. T., Wolf, A., Yahr, M. D., Harter, D. H., Duffy, P. E., Barden, H., and Hsu, K. C. (1974). Influenza virus antigen in postencephalitic parkinsonism brain. Detection by immunofluorescence. *Arch. Neurol.* **31,** 228–232.

Grunert, R. R., Mcgahen, J. W., and Davies, W. L. (1965). The *in vivo* antiviral activity of 1-adamantanamine (amantadine). 1. Prophylactic and therapeutic activity against influenza viruses. *Virology* **26,** 262–269.

Hakoda, S., and Nakatani, T. (2000). A pregnant woman with influenza A encephalopathy in whom influenza A/Hong Kong virus (H3) was isolated from cerebrospinal fluid. *Arch. Intern. Med.* **160,** 1041, 1045.

Hayase, Y., and Tobita, K. (1997). Probable post-influenza cerebellitis. *Intern. Med.* **36,** 747–749.

Ito, Y., Ichiyama, T., Kimura, H., Shibata, M., Ishiwada, N., Kuroki, H., Furukawa, S., and Morishima, T. (1999). Detection of influenza virus RNA by reverse transcription-PCR and proinflammatory cytokines in influenza-virus-associated encephalopathy. *J. Med. Virol.* **58,** 420–425.

James, S. L. (1995). Role of nitric oxide in parasitic infections. *Microbiol. Rev.* **59,** 533–547.

Kasai, T., Togashi, T., and Morishima, T. (2000). Encephalopathy associated with influenza epidemics. *Lancet* **355,** 1558–1559.

Kolski, H., Ford-Jones, E. L., Richardson, S., Petric, M., Nelson, S., Jamieson, F., Blaser, S., Gold, R., Otsubo, H., Heurter, H., and MacGregor, D. (1998). Etiology of acute childhood encephalitis at The Hospital for Sick Children, Toronto, 1994–1995. *Clin. Infect. Dis.* **26,** 398–409.

Markushin, S., Ghiasi, H., Sokolov, N., Shilov, A., Sinitsin, B., Brown, D., Klimov, A., and Nayak, D. (1988). Nucleotide sequence of RNA segment 7 and the predicted amino sequence of M1 and M2 proteins of FPV/Weybridge (H7N7) and WSN (H1N1) influenza viruses. *Virus Res.* **10,** 263–272.

McCullers, J. A., Facchini, S., Chesney, P. J., and Webster, R. G. (1999). Influenza B virus encephalitis. *Clin. Infect. Dis.* **28,** 898–900.

Messiha, F. S. (1989). Mouse strain-dependent effect of amantadine on motility and brain biogenic amines. *Arch. Int. Pharmacodyn. Ther.* **302,** 74–85.

Mizuguchi, M. (1997). Acute necrotizing encephalopathy of childhood: A novel form of acute encephalopathy prevalent in Japan and Taiwan. *Brain Dev.* **19,** 81–92.

Mori, I., Diehl, A. D., Chauhan, A., Ljunggren, H. G., and Kristensson, K. (1999). Selective targeting of habenular, thalamic midline and monoaminergic brainstem neurons by neurotropic influenza A virus in mice. *J. Neurovirol.* **5,** 355–362.

Mori, I., and Kimura, Y. (2000). Apoptotic neurodegeneration induced by

FIG. 8. Neuronal loss observed on day 28 after infection in the brain of amantadine-treated mice. SNC and VTA. (A) Neuronal loss was not evident in the brain of mice treated with amantadine according to therapeutic regimen 1. (B) Neuronal depletion was prominent in the brain of mice treated with amantadine based on therapeutic regimen 3. Arrows indicate examples of morphologically normal neurons. The scale bar represents 10 μm, common to A and B.

influenza A virus infection in the mouse brain. *Microbes Infect.* **2,** 1329–1334.

Mori, I., and Kimura, Y. (2001). Neuropathogenesis of influenza viruses. *Microbes Infect.* **3,** 475–479.

Morikawa, A., Kato, Y., Sugiyama, T., Koide, N., Chakravortty, D., Yoshida, T., and Yokochi, T. (1999). Role of nitric oxide in lipopolysaccharide-induced hepatic injury in D-galactosamine-sensitized mice as an experimental endotoxic shock model. *Infect. Immunol.* **67,** 1018–1024.

Murphy, A. M., and Hawkes, R. A. (1970). Neurological complications of influenza A2-Hong Kong-68 virus. *Med. J. Aust.* **2,** 511.

Oades, R. D., and Halliday, G. M. (1987). Ventral tegmental (A10) system: Neurobiology. 1. Anatomy and connectivity. *Brain Res.* **434,** 117–165.

Okabe, N., Yamashita, K., Taniguchi, K., and Inouye, S. (2000). Influenza surveillance system of Japan and acute encephalitis and encephalopathy in the influenza season. *Pediatr. Int.* **42,** 187–191.

Oxford, J. S., and Galbraith, A. (1980). Antiviral activity of amantadine: A review of laboratory and clinical data. *Pharmacol. Ther.* **11,** 181–262.

Pasquier, D. A., Kemper, T. L., Forbes, W. B., and Morgane, P. J. (1977). Dorsal raphe, substantia nigra and locus coeruleus: Interconnections with each other and the neostriatum. *Brain Res. Bull.* **2,** 323–339.

Price, J. L., and Powell, T. P. (1970). The mitral and short axon cells of the olfactory bulb. *J. Cell Sci.* **7,** 631–651.

Reiss, C. S., and Komatsu, T. (1998). Does nitric oxide play a critical role in viral infections? *J. Virol.* **72,** 4547–4551.

Ryan, M. M., Procopis, P. G., and Ouvrier, R. A. (1999). Influenza A encephalitis with movement disorder. *Pediatr. Neurol.* **21,** 669–673.

Shammah-Lagnado, S. J., Negrao, N., Silva, B. A., and Ricardo, J. A. (1987). Afferent connections of the nuclei reticularis pontis oralis and caudalis: A horseradish peroxidase study in the rat. *Neuroscience* **20,** 961–989.

Shipley, M. T., and Adamek, G. D. (1984). The connections of the mouse olfactory bulb: A study using orthograde and retrograde transport of wheat germ agglutinin conjugated to horseradish peroxidase. *Brain Res. Bull.* **12,** 669–688.

Spector, R. (1988). Transport of amantadine and rimantadine through the blood-brain barrier. *J. Pharmacol. Exp. Ther.* **244,** 516–519.

Sugaya, N. (2000). Influenza-associated encephalopathy in Japan: Pathogenesis and treatment. *Pediatr. Int.* **42,** 215–218.

Takahashi, M., Yamada, T., Nakajima, S., Nakajima, K., Yamamoto, T., and Okada, H. (1995). The substantia nigra is a major target for neurovirulent influenza A virus. *J. Exp. Med.* **181,** 2161–2169.

Takahashi, M., Yamada, T., Nakashita, Y., Saikusa, H., Deguchi, M., Kida, H., Tashiro, M., and Toyoda, T. (2000). Influenza virus-induced encephalopathy: Clinicopathologic study of an autopsied case. *Pediatr. Int.* **42,** 204–214.

Takeda, M., Pekosz, A., Shuck, K., Pinto, L. H., and Lamb, R. A. (2002). Influenza A virus M2 ion channel activity is essential for efficient replication in tissue culture. *J. Virol.* **76,** 1391–1399.

Thraenhart, O., Schley, G., and Kuwert, E. (1975). Isolation of influenza virus "A/Hong Kong/1/68 (H3N2)" from liquor cerebrospinalis of patients with CNS involvement. *Med. Klin.* **70,** 1910–1914.

Togashi, T., Matsuzono, Y., and Narita, M. (2000). Epidemiology of influenza-associated encephalitis-encephalopathy in Hokkaido, the northernmost island of Japan. *Pediatr. Int.* **42,** 192–196.

Umezawa, K., Akaike, T., Fujii, S., Suga, M., Setoguchi, K., Ozawa, A., and Maeda, H. (1997). Induction of nitric oxide synthesis and xanthine oxidase and their roles in the antimicrobial mechanism against *Salmonella typhimurium* infection in mice. *Infect. Immunol.* **65,** 2932–2940.

Urabe, M., Tanaka, T., Odagiri, T., Tashiro, M., and Tobita, K. (1993). Persistence of viral genes in a variant of MDBK cell after productive replication of a mutant of influenza virus A/WSN. *Arch. Virol.* **128,** 97–110.